Inorganic Chemistry

Article

pubs.acs.org/IC

Five-Coordinate Silicon(II) Compounds with Si−M Bonds (M = Cr, Mo, W, Fe): Bis[*N*,*N*′-diisopropylbenzamidinato(−)]silicon(II) as a Ligand in Transition-Metal Complexes

Konstantin Junold,[†] Johannes A. Baus,[†] Christian Burschka,[†] Thomas Vent-Schmidt,[‡]
Sebastian Riedel,*[,‡,§] and Reinhold Tacke*[,†]

[†]Institut für Anorganische Chemie, Universität Würzburg, Am Hubland, 97074 Würzburg, Germany

[‡]Institut für Anorganische und Analytische Chemie, Universität Freiburg, Albertstrasse 21, 79104 Freiburg im Breisgau, Germany

[§]Institut für Chemie und Biochemie, Freie Universität Berlin, Fabeckstrasse 34−36, 14195 Berlin, Germany

Supporting Information

ABSTRACT: Reaction of the donor-stabilized silylene **1** with $[Cr(CO)_6]$, $[Mo(CO)_6]$, $[W(CO)_6]$, or $[Fe(CO)_5]$ leads to the formation of the transition-metal silylene complexes **2**−**5**, which contain five-coordinate silicon(II) moieties with Si−M bonds (M = Cr, Mo, W, Fe). These compounds were characterized by NMR spectroscopic studies in the solid state and in solution and by crystal structure analyses. These experimental investigations were complemented by computational studies to gain insight into the bonding situation of **2**−**5**. The nature of the Si−M bonds is best described as a single bond.

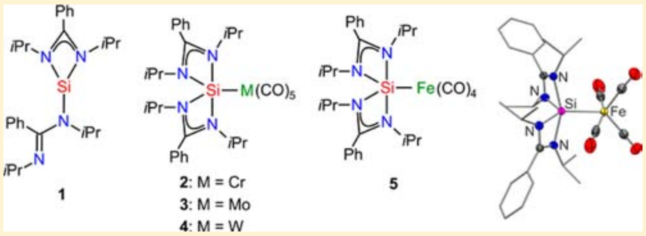

INTRODUCTION

The chemistry of stable silicon(II) compounds is currently one of the most actively studied fields in silicon chemistry.[1−4] Silicon(II) species (silylenes) show a very interesting reactivity profile; for example, they can behave as nucleophiles and therefore can act as ligands in transition-metal coordination chemistry.[5,6] In this context, stable N-heterocyclic silylene ligands play a special role.[1h] Recently, we have reported the synthesis of bis[*N*,*N*′-diisopropylbenzamidinato(−)]silicon(II) (**1**), a novel stable donor-stabilized three-coordinate silylene, and its nucleophilic substitution reaction with $[W(CO)_6]$ to form the tungsten silylene complex **4**, in which the silicon atom is five-coordinate.[4n] In continuation of these studies, we have now synthesized and characterized a series of further transition-metal complexes that also contain this particular silylene ligand, compounds **2**, **3**, and **5**. In addition, we have performed computational studies to gain some insight into the bonding situation of compounds **2**−**5**.

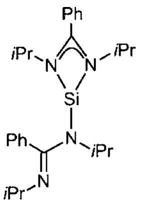

1

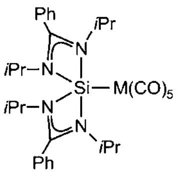

2: M = Cr
3: M = Mo
4: M = W

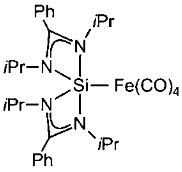

5

Herein we report (i) the synthesis and structural characterization of **2**, **3**, and **5**, (ii) the synthesis of **4**[4n] using a slightly modified method, and (iii) the computational characterization of the electronic structure of **2**−**5**. These investigations were performed as part of our systematic studies on higher-coordinate silicon(II) and silicon(IV) compounds (for recent publications, see refs 4n,o, and 6).

RESULTS AND DISCUSSION

Syntheses. Compounds **2**−**5** were synthesized by reaction of **1** with $[Cr(CO)_6]$, $[Mo(CO)_6]$, $[W(CO)_6]$, or $[Fe(CO)_5]$ at 20 °C (**2**, **4**, **5**) or 60 °C (**3**) in toluene (**2**, **5**) or THF (**3**, **4**) (Scheme 1; yields (**2**) 76%, (**3**) 89%, (**4**) 92%, (**5**) 65%). Compounds **2**−**4** were isolated as colorless crystalline solids, whereas **5** was obtained as a green-colored crystalline product. The identities of **2**−**5** were established by elemental analyses, NMR spectroscopic studies in the solid state (^{15}N, ^{29}Si) and in solution (^{1}H, ^{13}C, ^{29}Si), and crystal structure analyses (for the crystal structure analysis of **4**, see ref 4n).

The formation of **2**−**5** can be described as a nucleophilic substitution reaction, in which the silylene **1** formally reacts as a four-coordinate nucleophile that replaces one of the six (Cr, Mo, W) or five (Fe) carbonyl groups to give a five-coordinate silicon(II) species with an M−Si bond (M = Cr, Mo, W, Fe).

Crystal Structure Analyses. Compounds **2**, **3**, and **5** were structurally characterized by single-crystal X-ray diffraction. The crystal data and experimental parameters used for the crystal structure analyses are given in the Supporting Information (Table S1). The molecular structures of **2**, **3**, and **5** are depicted

Received: July 30, 2013
Published: September 24, 2013

Scheme 1. Syntheses of Compounds 2–5

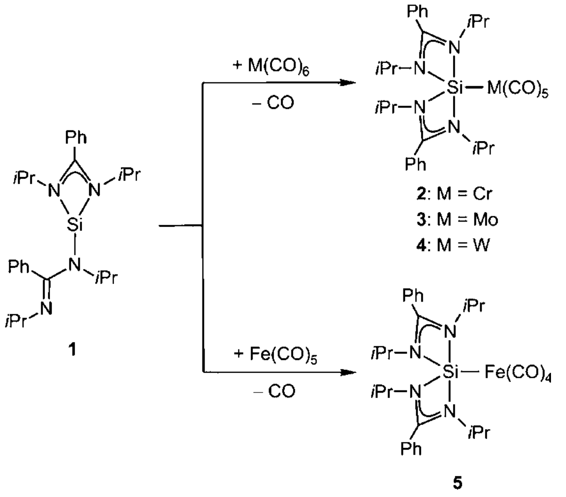

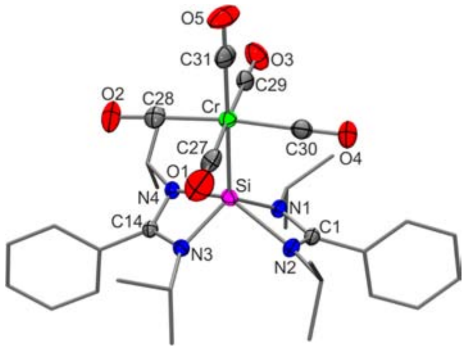

Figure 1. Molecular structure of **2** in the crystal (probability level of displacement ellipsoids 50%). Selected bond lengths (Å) and angles (deg): Cr–Si, 2.4181(7); Cr–C27, 1.879(2); Cr–C28, 1.887(2); Cr–C29, 1.879(2); Cr–C30, 1.880(2); Cr–C31, 1.853(2); Si–N1, 1.7982(17); Si–N2, 2.1567(19); Si–N3, 1.8014(17); Si–N4, 2.0825(17); N1–C1, 1.358(3); N2–C1, 1.307(3); N3–C14, 1.347(3); N4–C14, 1.314(2); C27–O1, 1.154(3); C28–O2, 1.146(3); C29–O3, 1.152(3); C30–O4, 1.150(3); C31–O5, 1.148(3); Si–Cr–C27, 90.59(7); Si–Cr–C28, 85.42(7); Si–Cr–C29, 89.41(7); Si–Cr–C30, 87.32(7); Si–Cr–C31, 179.07(8); C27–Cr–C28, 89.12(10); C27–Cr–C29, 178.54(10); C27–Cr–C30, 91.33(10); C27–Cr–C31, 88.97(10); C28–Cr–C29, 92.34(10); C28–Cr–C30, 172.73(9); C28–Cr–C31, 93.76(10); C29–Cr–C30, 87.21(9); C29–Cr–C31, 91.05(10); C30–Cr–C31, 93.51(10); Cr–Si–N1, 122.64(6); Cr–Si–N2, 107.13(5); Cr–Si–N3, 122.19(6); Cr–Si–N4, 108.22(5); N1–Si–N2, 66.14(7); N1–Si–N3, 115.11(8); N1–Si–N4, 95.11(7); N2–Si–N3, 92.88(7); N2–Si–N4, 144.64(7); N3–Si–N4, 67.27(7); N1–C1–N2, 109.70(17); N3–C14–N4, 108.85(16).

in Figures 1–3; selected bond lengths and angles are given in the respective figure captions.

For reasons of comparison, compound **4**[4n] is included in the discussion of the crystal structures of **2**, **3**, and **5**. The silicon coordination polyhedra of **2**–**5** are best described as strongly distorted trigonal bipyramids, with maximum deviations from the ideal 180° angles of 35.36° (**2**), 34.56° (**3**), 34.03° (**4**), and 25.36° (**5**). The sums of the equatorial bond angles of **2**–**5** amount to 359.9–360.0°, and the Berry distortions (transition trigonal bipyramid → square pyramid) were calculated at 36.8% (**2**), 34.4% (**3**), 34.8% (**4**), and 15.8% (**5**).[7] The transition-metal coordination polyhedra of **2**–**4** are best described as slightly distorted octahedra, with maximum deviations from the

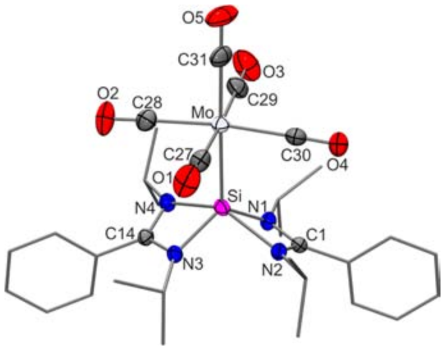

Figure 2. Molecular structure of **3** in the crystal (probability level of displacement ellipsoids 50%). Selected bond lengths (Å) and angles (deg): Mo–Si, 2.5784(6); Mo–C27, 2.039(2); Mo–C28, 2.041(2); Mo–C29, 2.032(2); Mo–C30, 2.039(2); Mo–C31, 2.000(2); Si–N1, 1.8101(15); Si–N2, 2.1417(15); Si–N3, 1.8052(15); Si–N4, 2.0894(15); N1–C1, 1.355(2); N2–C1, 1.300(2); N3–C14, 1.349(2); N4–C14, 1.309(2); C27–O1, 1.140(3); C28–O2, 1.142(2); C29–O3, 1.145(3); C30–O4, 1.144(3); C31–O5, 1.147(2); Si–Mo–C27, 91.63(6); Si–Mo–C28, 85.57(6); Si–Mo–C29, 90.23(6); Si–Mo–C30, 87.70(6); Si–Mo–C31, 178.70(7); C27–Mo–C28, 89.55(8); C27–Mo–C29, 177.42(8); C27–Mo–C30, 90.84(8); C27–Mo–C31, 87.60(9); C28–Mo–C29, 92.38(8); C28–Mo–C30, 173.27(8); C28–Mo–C31, 93.38(8); C29–Mo–C30, 87.45(8); C29–Mo–C31, 90.57(9); C30–Mo–C31, 93.35(8); Mo–Si–N1, 123.28(5); Mo–Si–N2, 107.24(5); Mo–Si–N3, 122.44(5); Mo–Si–N4, 107.32(5); N1–Si–N2, 66.00(6); N1–Si–N3, 114.26(7); N1–Si–N4, 95.13(6); N2–Si–N3, 93.58(6); N2–Si–N4, 145.44(6); N3–Si–N4, 67.05(6); N1–C1–N2, 109.63(15); N3–C14–N4, 108.96(14).

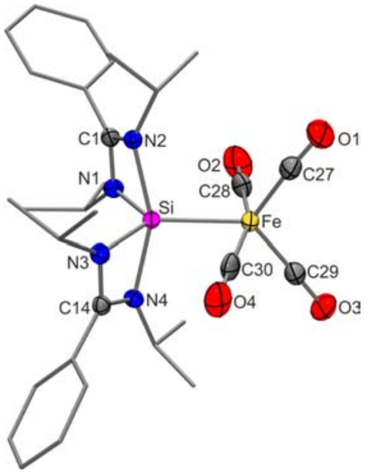

Figure 3. Molecular structure of **5** in the crystal (probability level of displacement ellipsoids 50%). Selected bond lengths (Å) and angles (deg): Fe–Si, 2.3175(6); Fe–C27, 1.7829(18); Fe–C28, 1.7655(19); Fe–C29, 1.7604(18); Fe–C30, 1.7605(19); Si–N1, 1.8201(13); Si–N2, 1.9569(13); Si–N3, 1.8247(14); Si–N4, 1.9864(13); N1–C1, 1.345(2); N2–C1, 1.3182(19); N3–C14, 1.347(2); N4–C14, 1.3149(19); C27–O1, 1.154(2); C28–O2, 1.155(2); C29–O3, 1.153(2); C30–O4, 1.159(2); Si–Fe–C27, 122.61(6); Si–Fe–C28, 79.51(6); Si–Fe–C29, 125.97(6); Si–Fe–C30, 79.11(6); C27–Fe–C28, 99.24(9); C27–Fe–C29, 111.40(8); C27–Fe–C30, 97.46(9); C28–Fe–C29, 94.06(9); C28–Fe–C30, 157.73(8); C29–Fe–C30, 93.46(9); Fe–Si–N1, 126.71(5); Fe–Si–N2, 102.29(4); Fe–Si–N3, 124.20(5); Fe–Si–N4, 103.05(4); N1–Si–N2, 69.01(5); N1–Si–N3, 109.09(6); N1–Si–N4, 94.68(6); N2–Si–N3, 97.74(6); N2–Si–N4, 154.64(6); N3–Si–N4, 68.51(5); N1–C1–N2, 107.10(12); N3–C14–N4, 107.69(13).

Table 1. Comparison of the Experimental Si−N Bond Lengths (Å) of **2**−**5**

compd	Si−N1	Si−N2	Si−N3	Si−N4	Δ_{max}[Si−N(eq)/Si−N(ax)]
2	1.7982(17)	2.1567(19)	1.8014(17)	2.0825(17)	0.3585
3	1.8101(15)	2.1417(15)	1.8052(15)	2.0894(15)	0.3365
4[a]	1.806(3)	2.081(3)	1.808(2)	2.129(3)	0.323
5	1.8201(13)	1.9569(13)	1.8247(14)	1.9864(13)	0.1663

[a] Data taken from ref 4n. The atomic numbering scheme for **4** is identical with that used for **2**, **3**, and **5**.

Table 2. Comparison of the Experimental M−Si and M−C Bond Lengths (Å) of **2**−**5** (M = Cr, Mo, W, Fe)

compd	M−Si	M−C27	M−C28	M−C29	M−C30	M−C31
2 (M = Cr)	2.4181(7)	1.879(2)	1.887(2)	1.879(2)	1.880(2)	1.853(2)
3 (M = Mo)	2.5784(6)	2.039(2)	2.041(2)	2.032(2)	2.039(2)	2.000(2)
4 (M = W)[a]	2.5803(9)	2.038(4)	2.037(3)	2.041(4)	2.039(3)	2.008(3)
5 (M = Fe)	2.3175(6)	1.7829(18)	1.7655(19)	1.7604(18)	1.7605(19)	

[a] Data taken from ref 4n. The atomic numbering scheme for **4** is identical with that used for **2**, **3**, and **5**.

ideal 90° and 180° angles ranging from 4.43° to 4.81° and from 6.73° to 7.27°, respectively. The iron coordination center of **5** is surrounded by its five ligand atoms in a distorted trigonal-bipyramidal fashion, with the silicon atom in an equatorial site. The axial C−Fe−C angle amounts to 157.73(8)°, and the sum of the equatorial bond angles is 360.0° (Berry distortion 32.8%).[7] It is interesting to note that the axial carbonyl ligands at the iron coordination center are bent toward the silicon atom, with Si−Fe−C angles of 79.51(6)° and 79.11(6)°. Such an "umbrella effect" is not observed for the carbonyl ligands *cis* to the silicon atom in compounds **2**−**4**.

As can be seen from Table 1, the axial Si−N bond distances of **2**−**5** (1.9569(13)−2.1567(19) Å) are longer than the equatorial ones (1.7982(17)−1.8247(14) Å). Interestingly, the maximum differences between the axial and equatorial Si−N distances of **2**−**4** (0.323−0.3585 Å) are quite similar, whereas this difference is much smaller for the iron complex **5** (0.1663 Å). Additionally, the equatorial Si−N bond lengths of **2**−**5** are quite similar (1.7982(17)−1.8247(14) Å), while the axial Si−N bond distances of **2**−**4** (2.081(3)−2.1567(19) Å) are considerably longer than those of the iron complex **5** (1.9569(13) Å and 1.9864(13) Å; Table 1). This may be interpreted by an overall weaker bonding of the amidinato ligands to the silicon coordination center of the group 6 complexes **2**−**4** compared to the iron complex **5**. However, this effect is not reflected by the N−C bond lengths within the NC(Ph)N moieties of **2**−**5**, which are very similar for all the complexes studied (C−N(eq), 1.345(2)−1.358(3) Å; C−N(ax), 1.300(2)−1.3182(19) Å), indicating a similar degree of electron delocalization within the NC(Ph)N moieties of **2**−**5**.

The M−Si bond distances of the molybdenum (**3**) and tungsten (**4**) silylene complexes are very similar (2.5784(6) Å and 2.5803(9) Å) and much longer than those found for the chromium (**2**) and iron (**5**) complexes (2.4181(7) Å and 2.3175(6) Å; Table 2). The M−Si bond distances of **2**−**5** are slightly longer than those reported for comparable complexes with three- or four-coordinate silylene ligands and M−Si single bonds, which is in line with the increase in the silicon coordination number from three or four to five.[8,9] As expected, the M−Si bond distances of **2**−**5** are markedly longer than those reported for transition-metal silylene complexes with Si═M double bonds (except ref 8i).[8,9]

In the six-coordinate transition-metal complexes **2**−**4**, the M−C bond distances (M = W, Cr, Mo) *trans* to the silicon atom are about 0.03−0.04 Å shorter than those in the *cis* position, indicating a rather small *trans* effect. In the five-coordinate iron complex **5**, the axial and equatorial Fe−C bond lengths are very similar (1.7604(18)−1.7829(18) Å), with the longest bond length observed for the equatorial Fe−C27 bond. The C−O bond lengths of **2**−**5** are very similar and range from 1.140(3) Å to 1.159(2) Å.

NMR Spectroscopic Studies. Compounds **2**, **3**, and **5** were studied by NMR spectroscopy in the solid state (^{15}N, ^{29}Si) and in solution (^{1}H, ^{13}C, ^{29}Si; solvent [D_8]THF). The data obtained (see the Experimental Section) confirm the identities of the compounds studied.

For reasons of comparison, compound **4**[4n] is included in the discussion of the NMR spectroscopic data of **2**, **3**, and **5**. As can be seen from Table 3, the respective isotropic ^{29}Si chemical shifts of **2**−**4** in the solid state and in solution are similar, indicating that these five-coordinate silicon(II) compounds also exist in solution. For compound **5**, the largest difference between the ^{29}Si chemical shifts in the solid state and in solution is found (11.0 ppm), indicating some change in geometry, however without a change in the silicon coordination number. The ^{29}Si chemical shifts depend on the transition metal bound to the silicon coordination center (solid state, δ = −23.7−4.9 ppm; solution, δ = −22.3−6.9 ppm). Compared to that of the donor-stabilized silylene **1** (three-coordinate in the solid state), the ^{29}Si resonance signals of **3** and **4** in the solid state show a low-field shift, while a high-field shift was observed for **2** and **5**. In solution, compounds **2**−**5** show ^{29}Si chemical shifts downfield compared to that of the silylene **1**. The molybdenum complex **3** shows the highest downfield shift of the ^{29}Si resonance signals in the solid state and in solution, which is in agreement with the results of the quantum-chemical calculations (see the Computational Studies).

Table 3. Comparison of the Isotropic ^{29}Si Chemical Shifts (ppm) of **1**−**5** in the Solid State (*T* = 22 °C) and in Solution [*T* = 23 °C, Solvent C_6D_6 (**1**) or [D_8]THF (**2**−**5**)]

compd	δ(^{29}Si) (solid state)	δ(^{29}Si) (solution)	compd	δ(^{29}Si) (solid state)	δ(^{29}Si) (solution)
1[a]	−15.4	−31.4	**4**[a]	−12.5	−13.3[b]
2	−22.3	−22.3	**5**	−23.7	−12.7
3	4.9	6.9			

[a] Data taken from ref 4n. [b] ^{183}W satellites: $^{1}J(^{29}\mathrm{Si},^{183}\mathrm{W})$ = 139.2 Hz.

As was found for other silicon(II) and silicon(IV) compounds with two amidinato ligands,[6c,d] compounds **2**−**5** show a dynamic behavior in solution at 23 °C. In the ^{1}H NMR spectra of these compounds only one doublet and one septet are observed for the four isopropyl groups of the two amidinato ligands. Accordingly, the ^{13}C{^{1}H} NMR spectra of **2**−**5** also show only one CH_3CHCH_3 and one CH_3CHCH_3 resonance signal. These findings can be explained by a rapid exchange of the amidinato-nitrogen binding sites of **2**−**5**.

As can be seen from Table 4, the ^{13}C chemical shifts of the carbonyl ligands of **2**−**4** strongly depend on the transition metal (δ = 203.3−227.3 ppm), but the shift differences between the *cis*- and *trans*-bound carbonyl ligands of a given transition metal are rather small ($\Delta\delta$ = 0.2−2.0 ppm). For the iron silylene complex **5**, only one resonance signal for the four carbonyl carbon atoms at δ = 220.4 ppm is observed in the ^{13}C{^{1}H} NMR spectrum.

Table 4. Comparison of the ^{13}C Chemical Shifts (ppm) of the Carbonyl Ligands of 2−4 in Solution (T = 23 °C, Solvent [D$_8$]THF)

compd	$\delta(^{13}C)$ (*cis*)	$\delta(^{13}C)$ (*trans*)	$\Delta\delta(^{13}C)$
2	225.3	227.3	2.0
3	213.9	213.7	0.2
4[a]	203.7	203.3	0.4

[a] Data taken from ref 4n.

Computational Studies. Compounds **2**−**4** were studied by quantum-chemical methods. The structural features of **2**−**5** obtained by structure optimizations at the PBE0/def-SV(P) level of theory (Tables 5 and 6) are in reasonable agreement with those obtained by the crystal structure analyses (Tables 2 and 3).

Table 5. Comparison of the Calculated Si−N Bond Lengths (Å) of 2−5 Obtained at the PBE0/def-SV(P) Level of Theory[a]

compd	Si−N1	Si−N2	Si−N3	Si−N4	Δ_{max}[Si−N(eq)/Si−N(ax)]
2	1.845	2.120	1.845	2.111	0.275
3	1.849	2.106	1.848	2.108	0.260
4	1.848	2.105	1.848	2.100	0.257
5	1.853	2.016	1.863	2.022	0.169

[a] The atomic numbering schemes for the calculated structures of **2**−**5** are identical with those used for the crystal structure analyses.

Table 6. Comparison of the Calculated M−Si and M−C Bond Lengths (Å) of 2−5 (M = Cr, Mo, W, Fe) Obtained at the PBE0/def-SV(P) Level of Theory[a]

compd	M−Si	M−C27	M−C28	M−C29	M−C30	M−C31
2 (M = Cr)	2.403	1.864	1.858	1.864	1.859	1.845
3 (M = Mo)	2.586	2.037	2.031	2.037	2.031	2.012
4 (M = W)	2.610	2.056	2.049	2.056	2.049	2.030
5 (M = Fe)	2.274	1.758	1.757	1.758	1.755	

[a] The atomic numbering schemes for the calculated structures of **2**−**5** are identical with those used for the crystal structure analyses.

Additionally, the isotropic ^{29}Si chemical shifts of **2**−**5** were calculated at the PBE0/def2-TZVPP level of theory: **2**, δ = −18.6 ppm; **3**, δ = 0.6 ppm; **4**, δ = −7.3 ppm; **5**, δ = −7.3 ppm. These computed gas-phase chemical shifts are in reasonable agreement with the experimental isotropic ^{29}Si chemical shifts both in the solid state and in solution (Table 3). In the case of **5**, the calculated chemical shift (δ = −7.3 ppm) is also in reasonable agreement with the experimental chemical shift in solution (δ = −12.7 ppm), whereas a difference of 16.4 ppm compared to the chemical shift in the solid state (δ = −23.7 ppm) is observed, indicating that the solid-state structure of **5** differs somewhat from the structure in solution.

Furthermore, on the basis of quantum-chemical calculations at the DFT level, we have investigated the nature of the chemical bonds between the silicon atom and the metal coordination centers. The nature of the Si−M bonds (M = Cr, Mo, W, Fe) in terms of a single or double bond can be analyzed at first principle by comparison of the experimental bond lengths with the predicted bond distances derived from the respective single bond and double bond radii listed in ref 10. For all compounds investigated, the values of the predicted single bond distances are in better agreement with the experimentally obtained M−Si bond lengths compared to the predicted double bond distances (Table 7). Beyond this first principle analysis, we have also investigated the nature of the Si−M bonds by Mayer bond orders (Table 7) and natural bond orbital (NBO) analyses (Table 8). Comparison of the Mayer bond orders reveals that the Si−Fe bond shows the lowest value (0.65), whereas the Mayer bond orders of the other three Si−M bonds are somewhat higher (0.71−0.78). Analysis of the molecular orbital (MO) ratios shows that the Si−Cr and Si−Mo bonds are almost equally shared between the silicon and transition-metal atom, whereas the silicon contribution in the Si−W and Si−Fe bonds is slightly higher. According to the NBO analyses, the contribution of the silicon atom is best described as 2/3 s and 1/3 p character (Table 8). Surprisingly, the main contribution of the transition-metal atoms originates from p orbitals with more than 50% participation and d orbital participation with 24.3−29.9%, whereas the remaining contribution comes from the s orbitals (Table 8). Selected molecular Kohn−Sham orbitals of compounds **2**−**5** that contribute to the silicon−metal and silicon−nitrogen bonds are depicted in Figure S1 in the Supporting Information. Furthermore, the calculation of the natural population analysis (NPA) charges shows that the silicon center is positively charged between 2.00 and 1.78, whereas the transition-metal atoms are always negatively charged, as expected. Note that the NPA charge of the chromium atom is much larger than that of the other transition-metal atoms (Table 7).

■ CONCLUSION

The donor-stabilized silylene **1** reacts with [$Cr(CO)_6$], [$Mo(CO)_6$], [$W(CO)_6$], and [$Fe(CO)_5$] as a nucleophile to give compounds **2**−**5**. With the synthesis of **2**−**5**, a new class of transition-metal silylene complexes has been made accessible. These compounds represent five-coordinate silicon(II) complexes with Si−M bonds (M = Cr, Mo, W, Fe), which, according to computational studies, are best described as single bonds. The structures of **2**−**5** in the solid state and in solution are very similar. The silicon coordination polyhedra of these compounds are strongly distorted trigonal bipyramids, with the transition metal in an equatorial position.

■ EXPERIMENTAL SECTION

General Procedures. All syntheses were carried out under dry argon. The organic solvents used were dried, purified, and deoxygenated according to standard procedures and stored under

Table 7. Bonding Analysis of the Si−M Bonds of **2**−**5** (M = Cr, Mo, W, Fe)[a]

compd	predicted single bond distance[b]	predicted double bond distance[b]	exptl bond distance	calcd bond distance[c]	Mayer bond order[d]	MO ratio, Si:M (%)	NPA charge, Si/M
2 (M = Cr)	2.38	2.18	2.418	2.403	0.71	50.4:49.6	2.00/−3.59
3 (M = Mo)	2.54	2.28	2.578	2.586	0.77	48.9:51.1	1.85/−2.62
4 (M = W)	2.53	2.27	2.580	2.610	0.78	55.5:44.5	1.78/−2.20
5 (M = Fe)	2.32	2.16	2.318	2.274	0.65	59.2:40.8	1.95/−2.59

[a] Bond distances in Å. [b] Data taken from ref 10. [c] Computed at the PBE0/def-SV(P) level of theory. [d] Computed at the PBE0/def2-TZVPP level of theory.

Table 8. NBO Analysis of the Si−M Bonds of **2**−**5** (M = Cr, Mo, W, Fe) at the PBE0/def2-TZVPP Level of Theory

	contribution of the Si orbitals to the Si−M bond (%)				contribution of the M orbitals to the Si−M bond (%)			
compd	s	p	d	f	s	p	d	f
2 (M = Cr)	71.8	28.1	0	0	17.4	52.7	29.9	0
3 (M = Mo)	67.7	32.2	0.1	0	17.3	56.8	25.8	0
4 (M = W)	65.2	34.7	0.1	0	17.3	55.1	27.6	0
5 (M = Fe)	66.6	33.2	0.2	0	13.6	62.1	24.3	0

argon. Solution ^{1}H, $^{13}\mathrm{C}\{^{1}\mathrm{H}\}$, and $^{29}\mathrm{Si}\{^{1}\mathrm{H}\}$ NMR spectra were recorded at 23 °C on a Bruker DRX-300 (^{1}H, 300.1 MHz; ^{13}C, 75.5 MHz; ^{29}Si, 59.6 MHz) or Bruker Avance 500 (^{1}H, 500.1 MHz; ^{13}C, 125.8 MHz; ^{29}Si, 99.4 MHz) NMR spectrometer using [D$_8$]THF as the solvent. Chemical shifts (ppm) were determined relative to internal [D$_7$]THF (^{1}H, δ = 1.73 ppm; [D$_8$]THF), internal [D$_8$]THF (^{13}C, δ = 25.3 ppm; [D$_8$]THF), or external TMS (^{29}Si, δ = 0 ppm; [D$_8$]THF). Assignment of the ^{1}H and ^{13}C NMR data was supported by DEPT 135 and ^{1}H−^{1}H and ^{1}H−^{13}C correlation experiments. Solid-state ^{15}N and ^{29}Si VACP/MAS NMR spectra were recorded at 22 °C on a Bruker DSX-400 NMR spectrometer with bottom layer rotors of $\mathrm{ZrO_2}$ (diameter 4 mm) containing ca. 80 mg of sample (^{15}N, 40.6 MHz; ^{29}Si, 79.5 MHz; external standard, glycine (^{15}N, δ = −342.0 ppm) or TMS (^{29}Si, δ = 0 ppm); spinning rate, 10 kHz; contact time, 3 ms (^{15}N) or 5 ms (^{29}Si); 90° ^{1}H transmitter pulse length, 2.6 μs; repetition time, 4−7 s). Elemental analyses were performed by using a VarioMicro apparatus (Elementar Analysensysteme GmbH).

Compound 2. Toluene (20 mL) was added in a single portion at 20 °C to a mixture of **1** (500 mg, 1.15 mmol) and chromium hexacarbonyl (254 mg, 1.15 mmol), and the reaction mixture was then stirred at this temperature for 16 h. The resulting solution was concentrated in vacuo to a volume of 2 mL, and the resulting suspension was heated until a clear solution was obtained, which was then cooled slowly to −20 °C and kept undisturbed at this temperature for 1 d. The resulting colorless crystalline solid was isolated by filtration, washed with *n*-pentane (2 × 5 mL), and dried in vacuo (20 °C, 4 h, 0.01 mbar). Yield: 549 mg (876 μmol, 76%). ^{1}H NMR (300.1 MHz): δ = 1.15 (d, $^{3}J(^{1}\mathrm{H},^{1}\mathrm{H})$ = 6.9 Hz, 24 H; $\mathrm{C}\mathit{H}_3\mathrm{CHC}\mathit{H}_3$), 3.82 (sept, $^{3}J(^{1}\mathrm{H},^{1}\mathrm{H})$ = 6.9 Hz, 4 H; $\mathrm{CH_3C}\mathit{H}\mathrm{CH_3}$), 7.46−7.55 (m, 10 H; $\mathrm{C_6}\mathit{H}_5$). $^{13}\mathrm{C}\{^{1}\mathrm{H}\}$ NMR (75.5 MHz): δ = 25.5 (8 C; $\mathit{C}\mathrm{H_3CH}\mathit{C}\mathrm{H_3}$), 49.3 (4 C; $\mathrm{CH_3}\mathit{C}\mathrm{HCH_3}$), 129.8 (4 C; *o*-$\mathrm{C_6H_5}$), 130.6 (4 C; *m*-$\mathrm{C_6H_5}$), 131.6 (2 C; *p*-$\mathrm{C_6H_5}$), 134.4 (2 C; *i*-$\mathrm{C_6H_5}$), 169.8 (2 C; NCN), 225.3 (4 C; *cis*-CO), 227.3 (1 C; *trans*-CO). $^{29}\mathrm{Si}\{^{1}\mathrm{H}\}$ NMR (59.6 MHz): δ = −22.3. ^{15}N VACP/MAS NMR: δ = −232.9, −226.9, −177.5, −162.3. ^{29}Si VACP/MAS NMR: δ = −22.3 (br s; fwhh = 223 Hz). Anal. Calcd for $\mathrm{C_{31}H_{38}CrN_4O_5Si}$ (626.75): C, 59.31; H, 6.11; N, 8.94. Found: C, 59.5; H, 6.2; N, 8.9.

Compound 3. THF (20 mL) was added in a single portion at 20 °C to a mixture of **1** (500 mg, 1.15 mmol) and molybdenum hexacarbonyl (304 mg, 1.15 mmol), and the reaction mixture was then stirred at 60 °C for 5 h. The resulting solution was concentrated in vacuo to a volume of 2 mL, cooled slowly to −20 °C, and then kept undisturbed at this temperature for 2 d. The resulting colorless crystalline solid was isolated by filtration, washed with *n*-pentane (2 × 5 mL), and dried in vacuo (20 °C, 4 h, 0.01 mbar). Yield: 687 mg (1.02 mmol, 89%). ^{1}H NMR (300.1 MHz): δ = 1.16 (d, $^{3}J(^{1}\mathrm{H},^{1}\mathrm{H})$ = 6.9 Hz, 24 H; $\mathrm{C}\mathit{H}_3\mathrm{CHC}\mathit{H}_3$), 3.77 (sept, $^{3}J(^{1}\mathrm{H},^{1}\mathrm{H})$ = 6.9 Hz, 4 H; $\mathrm{CH_3C}\mathit{H}\mathrm{CH_3}$), 7.42−7.54 (m, 10 H; $\mathrm{C_6}\mathit{H}_5$). $^{13}\mathrm{C}\{^{1}\mathrm{H}\}$ NMR (75.5 MHz): δ = 24.7 (8 C; $\mathit{C}\mathrm{H_3CH}\mathit{C}\mathrm{H_3}$), 48.2 (4 C; $\mathrm{CH_3}\mathit{C}\mathrm{HCH_3}$), 129.1 (4 C; *o*-$\mathrm{C_6H_5}$), 129.6 (4 C; *m*-$\mathrm{C_6H_5}$), 130.6 (2 C; *p*-$\mathrm{C_6H_5}$), 133.7 (2 C; *i*-$\mathrm{C_6H_5}$), 168.7 (2 C; NCN), 213.9 (4 C; *cis*-CO), 213.7 (1 C; *trans*-CO). $^{29}\mathrm{Si}\{^{1}\mathrm{H}\}$ NMR (59.6 MHz): δ = 6.9. ^{15}N VACP/MAS NMR: δ = −232.2, −228.8, −174.4, −163.0. ^{29}Si VACP/MAS NMR: δ = 4.9. Anal. Calcd for $\mathrm{C_{31}H_{38}MoN_4O_5Si}$ (670.69): C, 55.52; H, 5.71; N, 8.35. Found: C, 55.8; H, 5.5; N, 8.4.

Compound 4. This compound was synthesized according to ref 4n using a slightly modified method: THF (20 mL) was added at 20 °C in a single portion to a mixture of **1** (500 mg, 1.15 mmol) and tungsten hexacarbonyl (405 mg, 1.15 mmol), and the reaction mixture was then stirred at this temperature for 3 h. The solvent was removed in vacuo, and toluene (1.5 mL) was added to the residue. The solution was cooled slowly to −20 °C and then kept undisturbed at this temperature for 1 d. The resulting colorless crystalline solid was isolated by filtration, washed with *n*-pentane (2 × 5 mL), and dried in vacuo (20 °C, 6 h, 0.01 mbar). Yield: 804 mg (1.06 mmol, 92%). ^{1}H NMR (500.1 MHz): δ = 1.16 (d, $^{3}J(^{1}\mathrm{H},^{1}\mathrm{H})$ = 6.9 Hz, 24 H; $\mathrm{C}\mathit{H}_3\mathrm{CHC}\mathit{H}_3$), 3.77 (sept, $^{3}J(^{1}\mathrm{H},^{1}\mathrm{H})$ = 6.9 Hz, 4 H; $\mathrm{CH_3C}\mathit{H}\mathrm{CH_3}$), 7.46−7.54 (m, 10 H; $\mathrm{C_6}\mathit{H}_5$). $^{13}\mathrm{C}\{^{1}\mathrm{H}\}$ NMR (125.8 MHz): δ = 24.6 (8 C; $\mathit{C}\mathrm{H_3CH}\mathit{C}\mathrm{H_3}$), 48.1 (4 C; $\mathrm{CH_3}\mathit{C}\mathrm{HCH_3}$), 129.1 (4 C; *o*-$\mathrm{C_6H_5}$), 129.7 (4 C; *m*-$\mathrm{C_6H_5}$), 130.3 (2 C; *p*-$\mathrm{C_6H_5}$), 133.7 (2 C; *i*−$\mathrm{C_6H_5}$), 169.4 (2 C; NCN), 203.3 (1 C; ^{183}W satellites, $^{1}J(^{13}\mathrm{C},^{183}\mathrm{W})$ = 145.0 Hz; *trans*-CO), 203.7 (4 C; ^{183}W satellites, $^{1}J(^{13}\mathrm{C},^{183}\mathrm{W})$ = 123.1 Hz; *cis*-CO). $^{29}\mathrm{Si}\{^{1}\mathrm{H}\}$ NMR (99.4 MHz): δ = −13.3 (^{183}W satellites, $^{1}J(^{29}\mathrm{Si},^{183}\mathrm{W})$ = 139.2 Hz). ^{15}N VACP/MAS NMR: δ = −232.7, −229.6, −173.8, −163.0. ^{29}Si VACP/MAS NMR: δ = −12.5 (br). Anal. Calcd for $\mathrm{C_{31}H_{38}N_4O_5SiW}$ (758.59): C, 49.08; H, 5.05; N, 7.39. Found: C, 49.3; H, 5.0; N, 7.4.

Compound 5. Iron pentacarbonyl (225 mg, 1.15 mmol) was added in a single portion at 20 °C to a stirred solution of **1** (500 mg, 1.15 mmol) in toluene (20 mL), and the reaction mixture was then stirred at this temperature for 16 h. The resulting solution was concentrated in vacuo to a volume of 2 mL, and the resulting suspension was heated until a clear solution was obtained, which was then cooled slowly to −20 °C and kept undisturbed at this temperature for 1 d. The resulting green-colored crystalline solid was isolated by filtration, washed with *n*-pentane (2 × 5 mL), and dried in vacuo (20 °C, 4 h, 0.01 mbar). Yield: 450 mg (747 μmol, 65%). ^{1}H NMR (500.1 MHz): δ = 1.15 (d, $^{3}J(^{1}\mathrm{H},^{1}\mathrm{H})$ = 6.9 Hz, 24 H; $\mathrm{C}\mathit{H}_3\mathrm{CHC}\mathit{H}_3$), 3.85 (sept, $^{3}J(^{1}\mathrm{H},^{1}\mathrm{H})$ = 6.9 Hz, 4 H; $\mathrm{CH_3C}\mathit{H}\mathrm{CH_3}$), 7.48−7.58 (m, 10 H; $\mathrm{C_6}\mathit{H}_5$). $^{13}\mathrm{C}\{^{1}\mathrm{H}\}$ NMR (125.8 MHz): δ = 23.9 (8 C; $\mathit{C}\mathrm{H_3CH}\mathit{C}\mathrm{H_3}$), 47.8 (4 C; $\mathrm{CH_3}\mathit{C}\mathrm{HCH_3}$), 129.2 (4 C; *o*-$\mathrm{C_6H_5}$), 129.3 (4 C; *m*-$\mathrm{C_6H_5}$), 131.1 (2 C; *p*-$\mathrm{C_6H_5}$), 132.6 (2 C; *i*-$\mathrm{C_6H_5}$), 170.2 (2 C; NCN), 220.4 (4 C; CO). $^{29}\mathrm{Si}\{^{1}\mathrm{H}\}$ NMR (99.4 MHz): δ = −12.7. ^{15}N VACP/MAS NMR: δ = −229.4, −221.6, −190.4, −178.8. ^{29}Si VACP/MAS NMR: δ = −23.7. Anal. Calcd for $\mathrm{C_{30}H_{38}FeN_4O_4Si}$ (602.59): C, 59.80; H, 6.36; N, 9.30. Found: C, 59.6; H, 6.5; N, 9.3.

Crystal Structure Analyses. Suitable single crystals of **2**, **3**, and **5** were obtained as described in the subsections dealing with the syntheses. The crystals were mounted in inert oil (perfluoropolyalkyl ether, ABCR) on a glass fiber and then transferred to the cold nitrogen gas stream of the diffractometer (Stoe IPDS, graphite-monochromated Mo Kα radiation, λ = 0.71073 Å). The structures were solved by direct methods (SHELXS-97) and refined by full-matrix least-squares on F^2 for all unique reflections (SHELXL-97).[11] For the CH hydrogen atoms, a riding model was employed. CCDC 952145–952147 contain the supplementary data for this paper. These data can be obtained free of charge from The Cambridge Crystallographic Data Center via www.ccdc.com.ac.uk/data_request/cif.

Computational Studies. The structures of compounds **2**–**5** were fully optimized at the PBE0[12] hybrid DFT level of theory by using the Turbomole 6.4 program.[13] Quasirelativistic energy-adjusted pseudopotentials (effective core potentials, ECPs)[14] for the transition-metal atoms were employed as implemented in Turbomole,[12] together with the corresponding def-SV(P) basis set for each element.

NPA, NBO analyses,[15] and calculations of the Mayer bond orders[16] were performed by using the built-in modules of Gaussian 09[17] (single points at the PBE0/def2-TZVPP level of theory). Calculations of the isotropic chemical shifts were performed by using the Gaussian 09[17] program suite at the PBE0/def2-TZVPP level of theory.

■ ASSOCIATED CONTENT

Ⓢ Supporting Information

Crystallographic data for compounds **2**, **3**, and **5** (Table S1 and CIF files) and Figure S1 depicting selected molecular Kohn–Sham orbitals of compounds **2**–**5** that contribute to the silicon–metal and silicon–nitrogen bonds. This material is available free of charge via the Internet at http://pubs.acs.org.

■ AUTHOR INFORMATION

Corresponding Authors

*E-mail: sriedel@psichem.de.
*E-mail: r.tacke@uni-wuerzburg.de.

Notes

The authors declare no competing financial interest.

■ ACKNOWLEDGMENTS

S.R. thanks the Fonds der Chemischen Industrie (FCI) for financial support. R.T. thanks the Deutsche Forschungsgemeinschaft for financial support (Grant TA 75/16-1).

■ REFERENCES

(1) For selected reviews dealing with stable silicon(II) compounds, see: (a) Gerhus, B.; Lappert, M. F. *J. Organomet. Chem.* **2001**, *617*–*618*, 209–223. (b) Nagendran, S.; Roesky, H. W. *Organometallics* **2008**, *27*, 457–492. (c) Mizuhata, Y.; Sasamori, T.; Tokitoh, N. *Chem. Rev.* **2009**, *109*, 3479–3511. (d) Asay, M.; Jones, C.; Driess, M. *Chem. Rev.* **2011**, *111*, 354–396. (e) Yao, S.; Xiong, Y.; Driess, M. *Organometallics* **2011**, *30*, 1748–1767. (f) Sen, S. S.; Khan, S.; Samuel, P. P.; Roesky, H. W. *Chem. Sci.* **2012**, *3*, 659–682. (g) Ghadwal, R. S.; Azhakar, R.; Roesky, H. W. *Acc. Chem. Res.* **2013**, *46*, 444–456. (h) Blom, B.; Stoelzel, M.; Driess, M. *Chem.—Eur. J.* **2013**, *19*, 40–62.

(2) For selected papers dealing with stable two-coordinate silicon(II) compounds, see: (a) Denk, M.; Lennon, R.; Hayashi, R.; West, R.; Beljakov, A. V.; Verne, H. P.; Haaland, A.; Wagner, M.; Metzler, N. *J. Am. Chem. Soc.* **1994**, *116*, 2691–2692. (b) Gehrhus, B.; Lappert, M. F.; Heinicke, J.; Boese, R.; Bläser, D. *J. Chem. Soc., Chem. Commun.* **1995**, 1931–1932. (c) Gehrhus, B.; Hitchcock, P. B.; Lappert, M. F.; Heinicke, J.; Boese, R.; Bläser, D. *J. Organomet. Chem.* **1996**, *521*, 211–220. (d) West, R.; Denk, M. *Pure Appl. Chem.* **1996**, *68*, 785–788. (e) Heinicke, J.; Oprea, A.; Kindermann, M. K.; Karpati, T.; Nyulászi, L.; Veszprémi, T. *Chem.—Eur. J.* **1998**, *4*, 541–545. (f) Haaf, M.; Schmiedl, A.; Schmedake, T. A.; Powell, D. R.; Millevolte, A. J.; Denk, M.; West, R. *J. Am. Chem. Soc.* **1998**, *120*, 12714–12719. (g) Kira, M.; Ishida, S.; Iwamoto, T.; Kabuto, C. *J. Am. Chem. Soc.* **1999**, *121*, 9722–9723. (h) Driess, M.; Yao, S.; Brym, M.; van Wüllen, C.; Lentz, D. *J. Am. Chem. Soc.* **2006**, *128*, 9628–9629. (i) Zark, P.; Schäfer, A.; Mitra, A.; Haase, D.; Saak, W.; West, R.; Müller, T. *J. Organomet. Chem.* **2010**, *695*, 398–408. (j) Xiong, Y.; Yao, S.; Driess, M. *Chem.—Eur. J.* **2012**, *18*, 3316–3320. (k) Protchenko, A. V.; Birjkumar, K. H.; Dange, D.; Schwarz, A. D.; Vidovic, D.; Jones, C.; Kaltsoyannis, N.; Mountford, P.; Aldrige, S. *J. Am. Chem. Soc.* **2012**, *134*, 6500–6503. (l) Rekken, B. D.; Brown, T. M.; Fettinger, J. C.; Tuononen, H. M.; Power, P. P. *J. Am. Chem. Soc.* **2012**, *134*, 6504–6507. (m) Abe, T.; Tanaka, R.; Ishida, S.; Kira, M.; Iwamoto, T. *J. Am. Chem. Soc.* **2012**, *134*, 20029–20032.

(3) For selected papers dealing with stable higher-coordinate silicon(II) compounds, see: (a) Jutzi, P.; Kanne, D.; Krüger, C. *Angew. Chem.* **1986**, *98*, 163–164; *Angew. Chem., Int. Ed. Engl.* **1986**, *25*, 164. (b) Karsch, H. H.; Keller, U.; Gamper, S.; Müller, G. *Angew. Chem.* **1990**, *102*, 297–298; *Angew. Chem., Int. Ed. Engl.* **1990**, *29*, 295–296. (c) Jutzi, P.; Mix, A.; Rummel, B.; Schoeller, W. W.; Neumann, B.; Stammler, H. G. *Science* **2004**, *305*, 849–851. (d) Yao, S.; Brym, M.; van Wüllen, C.; Driess, M. *Angew. Chem.* **2007**, *119*, 4237–4240; *Angew. Chem., Int. Ed.* **2007**, *46*, 4159–4162. (e) Jutzi, P.; Leszczyńska, K.; Neumann, B.; Schoeller, W. W.; Stammler, H.-G. *Angew. Chem.* **2009**, *121*, 2634–2637; *Angew. Chem., Int. Ed.* **2009**, *48*, 2596–2599. (f) Ghadwal, R. S.; Roesky, H. W.; Merkel, S.; Henn, J.; Stalke, D. *Angew. Chem.* **2009**, *121*, 5793–5796; *Angew. Chem., Int. Ed.* **2009**, *48*, 5683–5686. (g) Filippou, A. C.; Chernov, O.; Schnakenburg, G. *Angew. Chem.* **2009**, *121*, 5797–5800; *Angew. Chem., Int. Ed.* **2009**, *48*, 5687–5690. (h) Xiong, Y.; Yao, S.; Driess, M. *J. Am. Chem. Soc.* **2009**, *131*, 7562–7563. (i) Ghadwal, R. S.; Roesky, H. W.; Merkel, S.; Stalke, D. *Chem.—Eur. J.* **2010**, *16*, 85–88. (j) Gao, Y.; Zhang, J.; Hu, H.; Cui, C. *Organometallics* **2010**, *29*, 3063–3065. (k) Li, J.; Merkel, S.; Henn, J.; Meindl, K.; Döring, A.; Roesky, H. W.; Ghadwal, R. S.; Stalke, D. *Inorg. Chem.* **2010**, *49*, 775–777. (l) Meltzer, A.; Inoue, S.; Präsang, C.; Driess, M. *J. Am. Chem. Soc.* **2010**, *132*, 3038–3046. (m) Filippou, A. C.; Chernov, O.; Blom, B.; Stumpf, K. W.; Schnakenburg, G. *Chem.—Eur. J.* **2010**, *16*, 2866–2872. (n) Rodriguez, R.; Gau, D.; Contie, Y.; Kato, T.; Saffon-Merceron, N.; Baceiredo, A. *Angew. Chem.* **2011**, *123*, 11694–11697; *Angew. Chem., Int. Ed.* **2011**, *50*, 11492–11495. (o) Wang, W.; Inoue, S.; Irran, E.; Driess, M. *Angew. Chem.* **2012**, *124*, 3751–3754; *Angew. Chem., Int. Ed.* **2012**, *51*, 3691–3694. (p) Leszczyńska, K.; Abersfelder, K.; Mix, A.; Neumann, B.; Stammler, H.-G.; Cowley, M. J.; Jutzi, P.; Scheschkewitz, D. *Angew. Chem.* **2012**, *124*, 6891–6895; *Angew. Chem., Int. Ed.* **2012**, *51*, 6785–6788.

(4) For selected papers dealing with stable higher-coordinate silicon(II) compounds with amidinato ligands, see: (a) So, C.-W.; Roesky, H. W.; Magull, J.; Oswald, R. B. *Angew. Chem.* **2006**, *118*, 4052–4054; *Angew. Chem., Int. Ed.* **2006**, *45*, 3948–3950. (b) So, C.-W.; Roesky, H. W.; Gurubasavaraj, P. M.; Oswald, R. B.; Gamer, M. T.; Jones, P. G.; Blaurock, S. *J. Am. Chem. Soc.* **2007**, *129*, 12049–12054. (c) Yang, W.; Fu, H.; Wang, H.; Chen, M.; Ding, Y.; Roesky, H. W.; Jana, A. *Inorg. Chem.* **2009**, *48*, 5058–5060. (d) Sen, S. S.; Roesky, H. W.; Stern, D.; Henn, J.; Stalke, D. *J. Am. Chem. Soc.* **2010**, *132*, 1123–1126. (e) Tavčar, G.; Sen, S. S.; Azhakar, R.; Thorn, A.; Roesky, H. W. *Inorg. Chem.* **2010**, *49*, 10199–10202. (f) Sen, S. S.; Hey, J.; Herbst-Irmer, R.; Roesky, H. W.; Stalke, D. *J. Am. Chem. Soc.* **2011**, *133*, 12311–12316. (g) Jana, A.; Leusser, D.; Objartel, I.; Roesky, H. W.; Stalke, D. *Dalton Trans.* **2011**, *40*, 5458–5463. (h) Azhakar, R.; Sarish, S. P.; Roesky, H. W.; Hey, J.; Stalke, D. *Inorg. Chem.* **2011**, *50*, 5039–5043. (i) Azhakar, R.; Ghadwal, R. S.; Roesky, H. W.; Wolf, H.; Stalke, D. *J. Am. Chem. Soc.* **2012**, *134*, 2423–2428. (j) Azhakar, R.; Ghadwal, R. S.; Roesky, H. W.; Wolf, H.; Stalke, D. *Chem. Commun.* **2012**, *48*, 4561–4563. (k) Azhakar, R.; Roesky, H. W.; Holstein, J. J.; Dittrich, B. *Dalton Trans.* **2012**, *41*, 12096–12100. (l) Samuel, P. P.; Azhakar, R.; Ghadwal, R. S.; Sen, S. S.; Roesky, H. W.; Granitzka, M.; Matussek, J.; Herbst-Irmer, R.; Stalke, D. *Inorg. Chem.* **2012**, *51*, 11049–11054. (m) Azhakar, R.; Pröpper, K.; Dittrich, B.; Roesky, H. W. *Organometallics* **2012**, *31*, 7586–7590. (n) Junold, K.; Baus, J. A.; Burschka, C.; Tacke, R. *Angew. Chem.* **2012**, *124*, 7126–7129; *Angew. Chem., Int. Ed.* **2012**, *51*, 7020–7023. (o) Junold, K.; Baus, J. A.; Burschka, C.; Auerhammer, D.; Tacke, R. *Chem.—Eur. J.* **2012**, *18*, 16288–16291.

(5) For selected reviews dealing with transition-metal silylene complexes, see: (a) Lickiss, P. D. *Chem. Soc. Rev.* **1992**, 271–279.

(b) Waterman, R.; Hayes, P. G.; Tilley, T. D. *Acc. Chem. Res.* **2007**, *40*, 712−719. (c) Reference 1h.

(6) For recent papers dealing with higher-coordinate silicon(iv) compounds, see: (a) Cota, S.; Beyer, M.; Bertermann, R.; Burschka, C.; Götz, K.; Kaupp, M.; Tacke, R. *Chem.—Eur. J.* **2010**, *16*, 6582−6589. (b) Metz, S.; Theis, B.; Burschka, C.; Tacke, R. *Chem.—Eur. J.* **2010**, *16*, 6844−6856. (c) Junold, K.; Burschka, C.; Bertermann, R.; Tacke, R. *Dalton Trans.* **2010**, *39*, 9401−9413. (d) Junold, K.; Burschka, C.; Bertermann, R.; Tacke, R. *Dalton Trans.* **2011**, *40*, 9844−9857. (e) Kobelt, C.; Burschka, C.; Bertermann, R.; Fonseca Guerra, C.; Bickelhaupt, F. M.; Tacke, R. *Dalton Trans.* **2012**, *41*, 2148−2162. (f) Junold, K.; Burschka, C.; Tacke, R. *Eur. J. Inorg. Chem.* **2012**, 189−193. (g) Theis, B.; Weiß, J.; Lippert, W. P.; Bertermann, R.; Burschka, C.; Tacke, R. *Chem.—Eur. J.* **2012**, *18*, 2202−2206. (h) Weiß, J.; Theis, B.; Metz, S.; Burschka, C.; Fonseca Guerra, C.; Bickelhaupt, F. M.; Tacke, R. *Eur. J. Inorg. Chem.* **2012**, 3216−3228. (i) Baus, J. A.; Burschka, C.; Bertermann, R.; Fonseca Guerra, C.; Bickelhaupt, F. M.; Tacke, R. *Inorg. Chem.* **2013**, *52*, 10664−10675.

(7) The Berry distortions were analyzed with PLATON: Spek, A. L. *Acta Crystallogr., Sect. D* **2009**, *65*, 148−155.

(8) For selected papers dealing with silylene complexes of group 6 metals, see: (a) Nakatsuji, H.; Ushio, J.; Yonezawa, T. *J. Organomet. Chem.* **1983**, *258*, C1−C4. (b) Corriu, R. J. P.; Chauhan, B. P. S.; Lanneau, G. F. *Organometallics* **1995**, *14*, 1646−1656. (c) Petri, S. H. A.; Eikenberg, D.; Neumann, B.; Stammler, H.-G.; Jutzi, P. *Organometallics* **1999**, *18*, 2615−2618. (d) Ueno, K.; Masuko, A.; Ogino, H. *Organometallics* **1999**, *18*, 2694−2699. (e) Schmedake, T. A.; Haaf, M.; Paradise, B. J.; Millevolte, J. A.; Powell, R. D.; West, R. *J. Organomet. Chem.* **2001**, *636*, 17−25. (f) Hirotsu, M.; Nunokawa, T.; Ueno, K. *Organometallics* **2006**, *25*, 1554−1556. (g) Sakaba, H.; Hirata, T.; Kabuto, C.; Kabuto, K. *J. Organomet. Chem.* **2007**, *692*, 402−407. (h) Takanashi, K.; Lee, V. Y.; Yokoyama, T.; Sekiguchi, A. *J. Am. Chem. Soc.* **2009**, *131*, 916−917. (i) Dannappel, K.; Nienhaus, R.; Schürmann, M.; Costisella, B.; Jurkschat, K. *Z. Anorg. Allg. Chem.* **2009**, *635*, 2126−2134. (j) Shinohara, A.; McBee, J.; Tilley, T. D. *Inorg. Chem.* **2009**, *48*, 8081−8083. (k) Reference 2i. (l) Sakaba, H.; Oike, H.; Arai, Y.; Kwon, E. *Organometallics* **2012**, *31*, 8172−8177. (m) Reference 4i. (n) Al-Rafia, I. S. M.; Malcom, A. C.; McDonald, R.; Ferguson, M. J.; Rivard, E. *Chem. Commun.* **2012**, *48*, 1308−1310.

(9) For selected papers dealing with iron silylene complexes, see: (a) Schmid, G.; Welz, E. *Angew. Chem.* **1977**, *89*, 823−824; *Angew. Chem., Int. Ed. Engl.* **1977**, *16*, 785−786. (b) Marinetti-Mignani, A.; West, R. *Organometallics* **1987**, *6*, 141−144. (c) Ueno, K.; Tobita, H.; Shimoi, M.; Ogino, H. *J. Am. Chem. Soc.* **1988**, *110*, 4092−4093. (d) Ueno, K.; Tobita, H.; Ogino, H. *J. Organomet. Chem.* **1992**, *430*, 93−104. (e) Bodensieck, U.; Braunstein, P.; Deck, W.; Faure, T.; Knorr, M.; Stern, C. *Angew. Chem.* **1994**, *106*, 2561−2564; *Angew. Chem., Int. Ed. Engl.* **1994**, *33*, 2440−2442. (f) Ueno, K.; Ito, S.; Endo, K.-i.; Tobita, H.; Inomata, S.; Ogino, H. *Organometallics* **1994**, *13*, 3309−3314. (g) Reference 9b. (h) Tobita, H.; Sato, T.; Okazaki, M.; Ogino, H. *J. Organomet. Chem.* **2000**, *611*, 314−322. (i) Reference 4c. (j) Ghadwal, R. S.; Azhakar, R.; Pröpper, K.; Holstein, J. J.; Dittrich, B.; Roesky, H. W. *Inorg. Chem.* **2011**, *50*, 8502−8508.

(10) (a) Pyykkö, P.; Atsumi, M. *Chem.—Eur. J.* **2009**, *15*, 186−197. (b) Pyykkö, P.; Atsumi, M. *Chem.—Eur. J.* **2009**, *15*, 12770−12779.

(11) Sheldrick, G. M. *Acta Crystallogr., Sect. A* **2008**, *64*, 112−122.

(12) (a) Dirac, P. A. M. *Proc. R. Soc. London* **1929**, *A123*, 714−733. (b) Slater, J. C. *Phys. Rev.* **1951**, *81*, 385−390. (c) Perdew, J. P.; Wang, Y. *Phys. Rev. B* **1992**, *45*, 13244−13249. (d) Perdew, J. P.; Burke, K.; Ernzerhof, M. *Phys. Rev. Lett.* **1996**, *77*, 3865−3868. (e) Perdew, J. P.; Ernzerhof, M.; Burke, K. *J. Chem. Phys.* **1996**, *105*, 9982−9985.

(13) Turbomole 6.4, a development of the University of Karlsruhe and Forschungszentrum Karlsruhe GmbH, Karlsruhe, 2011. http://www.turbomole.com.

(14) Andrae, D.; Haeussermann, U.; Dolg, M.; Stoll, H.; Preuss, H. *Theor. Chim. Acta* **1990**, *77*, 123−141.

(15) Reed, A. E.; Curtiss, L. A.; Weinhold, F. *Chem. Rev.* **1988**, *88*, 899−926.

(16) Mayer, I. *J. Comput. Chem.* **2007**, *28*, 204−221.

(17) Frisch, M. J.; Trucks, G. W.; Schlegel, H. B.; Scuseria, G. E.; Robb, M. A.; Cheeseman, J. R.; Scalmani, G.; Barone, V.; Mennucci, B.; Petersson, G. A.; Nakatsuji, H.; Caricato, M.; Li, X.; Hratchian, H. P.; Izmaylov, A. F.; Bloino, J.; Zheng, G.; Sonnenberg, J. L.; Hada, M.; Ehara, M.; Toyota, K.; Fukuda, R.; Hasegawa, J.; Ishida, M.; Nakajima, T.; Honda, Y.; Kitao, O.; Nakai, H.; Vreven, T.; Montgomery, Jr., J. A.; Peralta, J. E.; Ogliaro, F.; Bearpark, M.; Heyd, J. J.; Brothers, E.; Kudin, K. N.; Staroverov, V. N.; Kobayashi, R.; Normand, J.; Raghavachari, K.; Rendell, A.; Burant, J. C.; Iyengar, S. S.; Tomasi, J.; Cossi, M.; Rega, N.; Millam, J. M.; Klene, M.; Knox, J. E.; Cross, J. B.; Bakken, V.; Adamo, C.; Jaramillo, J.; Gomperts, R.; Stratmann, R. E.; Yazyev, O.; Austin, A. J.; Cammi, R.; Pomelli, C.; Ochterski, J. W.; Martin, R. L.; Morokuma, K.; Zakrzewski, V. G.; Voth, G. A.; Salvador, P.; Dannenberg, J. J.; Dapprich, S.; Daniels, A. D.; Farkas, Ö.; Foresman, J. B.; Ortiz, J. V.; Cioslowski, J.; Fox, D. J. Gaussian 09, revision A.1; Gaussian, Inc., Wallingford CT, 2009.